Check for updates

High-power stable continuous-wave single-longitudinal-mode Nd:YVO$_4$ laser at 1342 nm

YAYUN MA,[1] YUANJI LI,[1,2] JINXIA FENG,[1,2] AND KUANSHOU ZHANG[1,2,*]

[1]*State Key Laboratory of Quantum Optics and Quantum Optics Devices, Institute of Opto-Electronics, Shanxi University, Taiyuan 030006, China*
[2]*Collaborative Innovation Center of extreme Optics, Shanxi University, Taiyuan 030006, China*
*kuanshou@sxu.edu.cn

Abstract: A universal model about the sufficient condition of stable single-longitudinal-mode (SLM) operation is established and applied to the theoretical analysis of a high power unidirectional ring Nd:YVO$_4$ laser at 1342 nm with energy transfer upconversion and excited stimulated absorption taken into account. A stable continuous-wave SLM laser with 1342 nm power of 11.3 W and 671 nm power of 0.3 W is fabricated by optimizing the transmission of output coupler and the temperature of LiB3O5 crystal. Mode-hopping-free laser operation with a power stability better than ± 0.5% and a frequency fluctuation less than ± 88 MHz is achieved during a given three hours.

OCIS codes: (140.3460) Lasers; (140.3570) Lasers, single-mode; (140.3560) Lasers, ring; (140.3515) Lasers, frequency doubled; (140.3613) Lasers, upconversion.

References and links

1. J. F. Barry, D. J. McCarron, E. B. Norrgard, M. H. Steinecker, and D. DeMille, "Magneto-optical trapping of a diatomic molecule," Nature **512**(7514), 286–289 (2014).
2. The LIGO Scientific Collaboration, "A gravitational wave observatory operating beyond the quantum shot-noise limit," Nat. Phys. **7**(12), 962–965 (2011).
3. X. Su, C. Tian, X. Deng, Q. Li, C. Xie, and K. Peng, "Quantum entanglement swapping between two multipartite entangled states," Phys. Rev. Lett. **117**(24), 240503 (2016).
4. M. R. Huo, J. L. Qin, Z. Yan, X. Jia, and K. Peng, "Generation of two types of nonclassical optical states using an optical parametric oscillator with a PPKTP crystal," Appl. Phys. Lett. **109**(22), 221101 (2016).
5. N. Kretzschmar, U. Eismann, F. Sievers, F. Chevy, and C. Salomon, "2.4-watts second-harmonic generation in ppZnO:LN ridge waveguide for lithium laser cooling," Opt. Express **25**(13), 14840–14855 (2017).
6. A. Miffre, M. Jacquey, M. Büchner, G. Trénec, and J. Vigué, "Lithium atom interferometer using laser diffraction: description and experiments," Eur. Phys. J. D **33**(1), 99–112 (2005).
7. I. E. Olivares and I. A. González, "Diode laser absorption spectroscopy of lithium isotopes," Appl. Phys. B **122**(10), 252 (2016).
8. Y. Yan, H. L. Zhang, Y. Liu, J. Li, P. Sha, J. He, H. Zhang, and J. Xin, "End-pumped 20.2-W Nd:YVO$_4$ cw slab laser at 1342 nm with a hybrid resonator," Opt. Commun. **282**(15), 3124–3126 (2009).
9. M. Okida, M. Itoh, T. Yatagai, H. Ogilvy, J. Piper, and T. Omatsu, "Heat generation in Nd doped vanadate crystals with 1.34 µm laser action," Opt. Express **13**(13), 4909–4915 (2005).
10. F. A. Camargo, T. Z. Willette, T. Badr, N. U. Wetter, and J. J. Zondy, "Tunable single-frequency NdYVO$_4$ BiB$_3$O$_6$ ring laser at 671 nm," IEEE J. Quantum Electron. **46**(5), 804–809 (2010).
11. Y. H. Zheng, Y. J. Wang, C. D. Xie, and K. C. Peng, "Single-frequency Nd:YVO$_4$ laser at 671 nm with high-output power of 2.8 W," IEEE J. Quantum Electron. **48**(1), 67–72 (2012).
12. K. I. Martin, W. A. Clarkson, and D. C. Hanna, "Self-suppression of axial mode hopping by intracavity second-harmonic generation," Opt. Lett. **22**(6), 375–377 (1997).
13. S. Greenstein and M. Rosenbluh, "The influence of nonlinear spectral bandwidth on single longitudinal mode intra-cavity second harmonic generation," Opt. Commun. **248**(1–3), 241–248 (2005).
14. H. Lu, J. Su, Y. Zheng, and K. Peng, "Physical conditions of single-longitudinal-mode operation for high-power all-solid-state lasers," Opt. Lett. **39**(5), 1117–1120 (2014).
15. L. Fornasiero, S. Kück, T. Jensen, G. Huber, and B. H. T. Chai, "Excited state absorption and stimulated emission of Nd^{3+} in crystals. Part 2: YVO$_4$, GdVO$_4$, and Sr$_5$(PO$_4$)$_3$F," Appl. Phys. B **67**(5), 549–553 (1998).
16. Y. F. Chen, L. J. Lee, T. M. Huang, and C. L. Wang, "Study of high-power diode-end-pumped Nd:YVO$_4$ laser at 1.34 µm: influence of Auger upconversion," Opt. Commun. **163**(4–6), 198–202 (1999).
17. X. Délen, F. Balembois, O. Musset, and P. Georges, "Characteristics of laser operation at 1064 nm in Nd:YVO$_4$ under diode pumping at 808 and 914 nm," J. Opt. Soc. Am. B **28**(1), 52–57 (2011).
18. R. Sarrouf, T. Badr, and J. J. Zondy, "Intracavity second-harmonic generation of diode-pumped continuous-wave, single-frequency 1.3 µm Nd:YLiF$_4$ lasers," J. Opt. A, Pure Appl. Opt. **10**(10), 104011 (2008).

19. G. C. Bowkett, G. W. Baxter, D. J. Booth, T. Taira, H. Teranishi, and T. Kobayashi, "Single-mode 1.34-μm Nd:YVO$_4$ microchip laser with cw Ti:sapphire and diode-laser pumping," Opt. Lett. **19**(13), 957–959 (1994).

1. Introduction

Solid state continuous wave (cw) single-longitudinal-mode (SLM) lasers have attracted great interest due to their excellent properties of high output power, low noise and good beam quality. This kind of laser is widely used in a variety of application fields, such as cold atom physics, precise measurements, quantum optics, and so on [1–3]. In particular, a high power 1342 nm laser stably operated in SLM state is highly desired in quantum information [4] and the generation of high power SLM 671 nm lasers, which are in demand for the optical cooling and trapping of lithium [5], lithium atom interferometers [6] and lithium isotope separation [7].

Comparing with the solid state lasers at 1064 nm, the 1342 nm lasers suffer from severer thermal effects originated from the large quantum defect and extra nonradiative transitions involved in the energy transfer upconversion (ETU) and excited stimulated absorption (ESA) [8,9], as well as smaller emission cross-section. As a consequence, stable SLM operation at 1342 nm is quite difficult to be achieved, especially when high output power is required. F. A. Camargo *et al*. reported a 1342 nm Nd:YVO$_4$ laser using a unidirectional ring cavity configuration and an output coupler (OC) with transmission of 2% [10]. There exist two or three modes oscillating simultaneously at a pump power of 10.5 W. Even though at a pump power of 9.7 W and inserting an etalon to help mode selection, the laser could be SLM operated during only half an hour. Y. H. Zheng *et al*. built a 1342 nm Nd:YVO$_4$ laser at a pump power of 23.5 W and output transmission of 8%, and found that the SLM operation can only maintained for a few seconds and then the mode hopping or multi-longitudinal-mode (MLM) operation occurred [11]. When the transmission of OC was 0.5% and a LiB3O5 (LBO) crystal was inserted for intracavity second harmonic generation (ICSHG), the red laser was stably operated in SLM state at perfect phase matching condition. Recently, N. Kretzschmar *et al*. demonstrated a SLM 1342 nm Nd:YVO$_4$ laser that generated output power of 6.6 W [5]. The high SLM output was obtained mainly depending on using two uncoated intracavity etalons and 888 nm direct pumping. However, uncoated intracavity etalons not only lower the output power by their insertion loss, but also degrade the laser stability due to that they are sensitive to temperature variation. It is known that introducing nonlinear loss via ICSHG is an effective approach to suppress mode hopping and thus improve the stability of a SLM laser [12–14], but how to suppress MLM operation at a high pump power and obtain high power stable SLM lasers was seldom investigated, especially for 1342 nm lasers, to the best of our knowledge.

In this paper, the sufficient conditions of stable SLM operation for cw all-solid-state lasers are investigated theoretically, especially for high power 1342 nm lasers with ETU and ESA taken into account. Based on the theoretical analysis, a high power cw SLM Nd:YVO$_4$ laser at 1342 nm is fabricated and the laser output characteristics are studied experimentally in detail.

2. Theoretical analysis

For an all-solid-state laser based on an ideal homogeneous broadening gain medium, SLM operation can be achieved via mode competition when a unidirectional ring cavity configuration is used. However, when lasers are operated at high pump power and with large cavity losses, owing to the influences of the serious thermal effects, the nonuniformly doping of gain medium and so on, some of the modes adjacent to the mode at gain line center will no longer be suppressed and the lasers will be MLM operated. Previous investigations suggested that introducing nonlinear loss via ICSHG can help the suppression of mode hopping in a single-frequency laser, which method can also be employed for the suppression of MLM oscillation in a high power unidirectional ring laser.

In the case that a unidirectional ring laser is MLM operated, we assume there are $2m$ modes at frequencies of $\omega_q = \omega_0 \pm q\Delta\omega$ ($q = 1, 2, \ldots, m$) oscillated together with the mode at center frequency (ω_0). $\Delta\omega$ is the longitudinal-mode-spacing of the laser. The small signal gain coefficient of mode ω_q can be written as

$$g_0(q) = g_0^{max} \Big/ \left[1 + \left(\frac{q \cdot \Delta\omega}{\Delta\omega_g / 2}\right)^2\right], \qquad (1)$$

where $g^{max} 0$ is the small signal gain coefficient at ω_0, $\Delta\omega_g$ is the gain bandwidth of the gain medium. In other words, if the net gain of a mode is smaller than the difference between the net gain of mode ω_0 and ΔG, the oscillation of this mode can be suppressed, where $\Delta G = [g^{max} 0 - g_0(m)]l_0$, l_0 is the length of the gain medium.

When a nonlinear crystal is inserted into the ring laser cavity, the processes of SHG and sum frequency generation (SFG) will introduce nonlinear losses of the fundamental wave due to the nonlinear conversion. If the difference of net gain between mode ω_0 and mode ω_1 can be enlarged by the frequency dependent nonlinear loss to a value that is larger than ΔG, and the net gain of mode ω_0 reaches the threshold condition simultaneously, MLM oscillation can be suppressed in a unidirectional ring laser. The sufficient condition of stable SLM operation can be written as

$$2K(\omega_0, \omega_1, \Delta\omega_{NL}) I(\omega_1) + K(\omega_0, \omega_0, \Delta\omega_{NL}) I(\omega_0) + \delta_0 + T_{oc} = \frac{g_0^{max} l_0}{1 + \frac{I(\omega_0)}{I_0(\omega_0)} + \frac{I(\omega_1)}{I_0(\omega_1)}}, \quad (2)$$

$$[g_0^{max} - g_0(1)]l_0 \Big/ (1 + \frac{I(\omega_0)}{I_0(\omega_0)} + \frac{I(\omega_1)}{I_0(\omega_1)}) - [2K(\omega_0, \omega_1, \Delta\omega_{NL}) I(\omega_1) + K(\omega_0, \omega_0, \Delta\omega_{NL}) I(\omega_0)$$
$$-2K(\omega_0, \omega_1, \Delta\omega_{NL}) I(\omega_0) - K(\omega_1, \omega_1, \Delta\omega_{NL}) I(\omega_1)] > \Delta G(m),$$
$$(3)$$

where δ_0 is the roundtrip dissipative loss, T_{oc} is the transmission of the OC, and $\Delta\omega_{NL}$ is the nonlinear spectral bandwidth of the nonlinear crystal. $K(\omega_i, \omega_i, \Delta\omega_{NL})$ and $K(\omega_i, \omega_j, \Delta\omega_{NL})$ ($i,j = \{0,1\}$) are the nonlinear conversion coefficients of SHG and SFG, respectively. $K(\omega_i, \omega_j, \Delta\omega_{NL})$ can be given by [13]

$$K(\omega_i, \omega_j, \Delta\omega_{NL}) = K \, \text{sinc}^2\left(1.39\frac{\omega_i + \omega_j - 2\omega_0}{\Delta\omega_{NL}}\right), \qquad (4)$$

and K is the simplified expression of $K(\omega_i, \omega_i, \Delta\omega_{NL})$. The right hand side of Eq. (2) is the large signal gain of mode ω_0 at high pump power. $I_0(\omega_i)$ is the saturated intensity of mode ω_i that can be calculated by

$$I_0(\omega_i) = I_0\left(1 + \left(\frac{i\Delta\omega}{\Delta\omega_g / 2}\right)^2\right), \qquad (5)$$

where $I_0 = h\nu_l / \sigma_e \tau$ is the saturated intensity of mode ω_0, $h\nu_l$ is the energy of laser photon, σ_e is the stimulated emission cross-section, τ is the fluorescence lifetime of the metastable level. $I(\omega_0)$ and $I(\omega_1)$ are the intensities of mode ω_0 and mode ω_1. Based on the observation in our experiment, $I(\omega_0)$ is significantly higher than $I(\omega_1)$, we can assume $I(\omega_0) \gg I(\omega_1)$ in the following analysis for the simplicity.

Using Eqs. (1)-(5), the sufficient condition of stable SLM operation for a high power unidirectional ring laser comes to be

$$AKI^2(\omega_0) + AKI_0 I(\omega_0) - Bg_0^{max} l_0 I(\omega_0) > CI_0 g_0^{max} l_0, \tag{6}$$

where

$$A = 2\sin c^2\left(1.39\frac{\Delta\omega}{\Delta\omega_{NL}}\right) - 1; \; B = \frac{(m\Delta\omega)^2}{(\Delta\omega_g/2)^2 + (m\Delta\omega)^2};$$

$$C = \frac{(m^2-1)\Delta\omega^2(\Delta\omega_g/2)^2}{\left((\Delta\omega_g/2)^2 + \Delta\omega^2\right)\left((\Delta\omega_g/2)^2 + m^2\Delta\omega^2\right)}. \tag{7}$$

The output powers of fundamental and second harmonic waves can be represented by

$$P_f = T_{oc} SI(\omega_0), \tag{8}$$

$$P_{sh} = K_0 SI^2(\omega_0), \tag{9}$$

where S is average transverse cross-section of fundamental laser beam inside the gain medium.

For a high-power diode-end-pumped Nd:YVO$_4$ laser at 1342 nm, the stimulated emission cross-section is smaller than that at 1064 nm, and detrimental energy processes, such as ESA and ETU, will reduce the effective stimulated emission cross-section [15] and the upper-state population density [16]. The average small signal gains with and without ETU and ESA can be given as [17]

$$\left(g_0^{max} l_0\right)_{etu\&esa} = \left(\sigma_e - \sigma_{esa}^l\right)\int_0^{l_0} n_{etu\&esa}(z)dz, \tag{10}$$

$$\left(g_0^{max} l_0\right)_{no\,etu\&esa} = \sigma_e\int_0^{l_0} n_{no\,etu\&esa}(z)dz, \tag{11}$$

respectively, where σ_{esa}^l is the ESA cross section at laser wavelength. $n_{etu\&esa}$ and $n_{no\,etu\&esa}$ are the population inversion densities with and without ETU and ESA taken into account that can be written as [16]

$$n_{etu\&esa} = \frac{\sqrt{1 + 4\gamma^2\tau^2 P_{in}\alpha\exp(-\alpha z)/\left(h\nu_p\pi w_{pa}^2\right)} - 1}{2\gamma\tau}, \tag{12}$$

$$n_{no\,etu\&esa} = P_{in}\tau\alpha\exp(-\alpha z)/\left(h\nu_p\pi w_{pa}^2\right), \tag{13}$$

respectively, where γ is the ETU coefficient, P_{in} is the incident pump power, α is the absorption coefficient of laser crystal at pump wavelength, $h\nu_p$ is the energy of pump photon, w_{pa} is the average pump beam radius in the gain medium.

Considering a high-power Nd:YVO$_4$ ring laser at 1342 nm end-pumped by a laser diode (LD) with the center wavelength of 880 nm and intracavity frequency doubled using a type-I critical phase-matched LBO crystal, with the parameters of P_{in} = 50 W, l_0 = 17 mm, cavity length L = 490 mm, and length of LBO l_{LBO} = 18 mm, the critical value of K as a function of T_{oc} for the sufficient condition of stable SLM operation is calculated using Eqs. (2)-(7) and (10)-(13) and the following parameters: α = 1.52 cm^{-1} (measured in experiment), τ = 100 μs [16], w_{pa} = 515 μm, δ_0 = 0.037, σ_e = 4.5*10^{-19} cm^2 [15], $\sigma l\,esa$ = 0.5*10^{-19} cm^2 [15], γ = 0.45*10^{-15} cm^3/s [17], $\Delta\omega_{NL}$ = 4405 GHz [18], $\Delta\omega_g$ = 266.5 GHz [19], $\Delta\omega$ = 613 MHz and m = 6 (since 13 longitudinal modes was observed in experiments), as shown in Fig. 1. Curves

(a) and (b) are the critical values of K versus T_{oc} with and without ETU and ESA, respectively. When K is located in the region above the curves, the laser can stably operate in SLM state, otherwise MLM will oscillate. It can be seen that the critical value of K which makes the laser in SLM operation is increased with increasing T_{oc}. Comparing with the case that ETU and ESA are not considered, at a given T_{oc}, larger value of K is required to ensure stable SLM operation when ETU and ESA are taken into account. For instance, when $T_{oc} =$ 18%, the maximum nonlinear conversion coefficient of $6.7*10^{-12}$ m^2/W achieved by perfect phase matching, which is denoted by the dashed line in Fig. 1, is enough for stable SLM selection in the absence of ETU and ESA, but the sufficient condition of stable SLM operation cannot be satisfied in the presence of ETU and ESA. According to the calculation, the critical values of K to make the laser SLM operated should be $2.04*10^{-12}$ m^2/W, $2.93*10^{-12}$ m^2/W and $3.89*10^{-12}$ m^2/W at a given T_{oc} of 4%, 7%, and 10%, respectively.
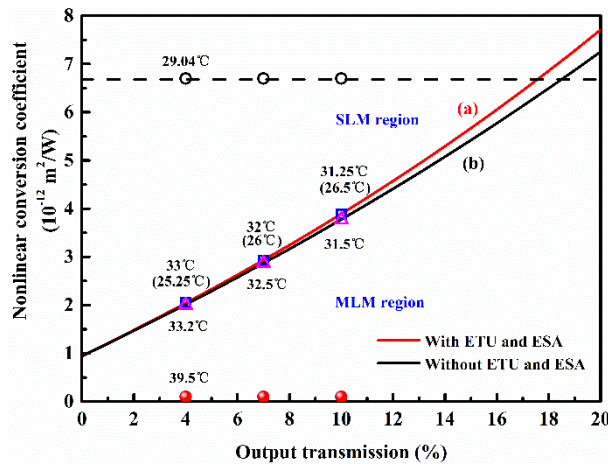

Fig. 1. Critical value of nonlinear conversion coefficient as a function of output transmission for the sufficient condition of stable SLM operation for a high-power cw laser at 1342 nm
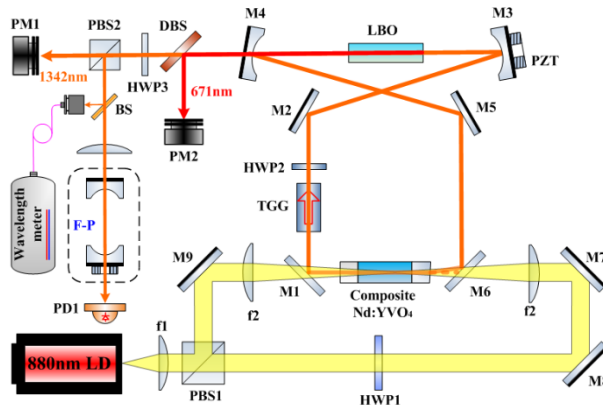
3. Experimental setup

Fig. 2. Experimental setup of a LD-pumped cw SLM Nd:YVO$_4$ laser at 1342 nm.

The experimental setup of a LD-pumped cw SLM Nd:YVO$_4$ laser at 1342 nm is shown in Fig. 2. The pump source is a commercially available LD (Model: LIMO60-F400-DL880-EX1124, LIMO) with center wavelength of 880 nm and a maximal output power of 60 W. Pump light passing through a fiber with core diameter of 400 μm and a collimated lens (f1) is spitted into two beams with orthogonal polarizations by a polarizing beam splitter (PBS1).

The transmitted pump beam whose polarization is rotated 90 degree by a half-wave plate (HWP1) and the reflected pump beam are both focused into the gain medium via two identical focusing lenses (f2). The gain medium is a composite a-cut Nd:YVO$_4$ crystal with a cross section of 3×3 mm^2 and a length of 27 mm, including two undoped end caps of 5 mm and Nd-doped central portion of 17 mm with the Nd concentration of 0.27at.%. Both end-faces of the Nd:YVO$_4$ crystal are anti-reflection (AR) coated at 880 nm and 1342 nm (R_{880nm} < 3% & R_{1342nm} < 0.2%). To suppress the oscillation of the σ-polarization mode and eliminate the etalon effect, a wedge shape of 1.5 degree is cut on one of the end-faces of the crystal with respect to the c-axis of the crystal. For longitudinal mode selection, a ring resonator composed of 6 mirrors (M1-M6) and an optical diode formed by HWP2 and a terbium gallium garnet (TGG) Faraday rotator is employed. The four plane mirrors (M1-M2, M5-M6) are high reflection (HR) coated at 1342 nm and high transmission (HT) coated at 880 nm and 1064 nm (45°, R_{1342nm} > 99.8% & $T_{880\&1064nm}$ > 95%). M3 and M4 are concave mirrors with curvature radii of 100 mm, where M3 is HR coated at 1342 nm (R_{1342nm} > 99.8%) and fixed onto a pizeoelectric-transducer (PZT), M4 acting as OC is partially transmission coated at 1342 nm. To introduce intracavity nonlinear loss via ICSHG, a LBO crystal cut for type-I critical phase-matching in the principle plane XZ ($\theta = 86.1°, \varphi = 0°$) with dimensions of $3 \times 3 \times 18$ mm^3 is used and placed at the center of the M3-M4 arm. Both end-faces of the LBO crystal are AR coated at 1342 nm and 671 nm (R_{1342nm} < 0.2% & R_{671nm} < 0.5%). Both the Nd:YVO$_4$ and LBO crystals are tightly wrapped with indium for reliable heat transfer and mounted in temperature controlled copper ovens. The value of K can be controlled by tuning the temperature of the LBO crystal. The whole cavity length is 490 mm.

The outputs of fundamental and second harmonic lasers are seperated using a dichroic mirror (DBS). The fundamental laser is splitted into three parts using HWP3, PBS2 and a beam splitter (BS). One small portion is delivered to a scanning Fabry-Perot (F-P) interferometer (free spectral range: 750 MHz; finesse: 370) for monitoring the longitudinal-mode. Another small portion is delivered to a wavelength meter with a resolution of 0.1 pm (Model:WS6-771, HighFinesse) for measuring the laser frequency. The powers of the main portion of fundamental laser and the second harmonic laser are measured using power meters (PM1 and PM2, Model:LabMax-Top, Coherent) simultaneously.

4. Experimental results and discussions

The output characteristics of LD-pumped cw Nd:YVO$_4$ lasers at 1342 nm were investigated at an incident pump power of 50 W, different output transmissions of 4%, 7% and 10%, and different temperatures of LBO. The measured output powers of 1342 nm and 671 nm lasers and the transmitted intensity of the scanned F-P interferometer at an output transmission of 7% and different LBO temperatures are shown in Fig. 3 and Fig. 4, respectively. When the temperature of LBO was controlled at 39.5 °C leading to a large phase mismatch, there was only 1342 nm output with a power of 10.8 W and the laser was in MLM operation with thirteen longitudinal modes oscillating simultaneously, as shown in Fig. 4(a) and by the ball in Fig. 1. With the decrease of the LBO temperature, the observed number of oscillated longitudinal mode was reduced. When the temperature of LBO was controlled at 32.5 °C leading to an imperfect phase match, the 1342 nm and 671 nm output powers were 11.27 W and 0.135 W, respectively, and there were two oscillated longitudinal modes, as shown in Fig. 4(b) and by the triangle in Fig. 1. When the temperature of LBO was controlled at 32 °C, there was one oscillated longitudinal mode, as shown in Fig. 4(c), but mode hopping occurred frequently. Owing to the laser is SLM operated, the output power at 1342 nm was steeply raised up to 11.42 W, and the output power at 671 nm was increased to 0.141 W, as shown in Fig. 3. According to the experimental data, the nonlinear conversion coefficient of ICSHG was nearly $3.0*10^{-12}$ m^2/W that approaches the calculated critical value of K for the sufficient condition of SLM operation, which is denoted by the square shown in Fig. 1. When the LBO temperature was tuned from 32 °C to 29.04 °C, the laser was in stable SLM operation, as

shown in Fig. 4(c), the output power at 1342 nm was reduced from 11.42 W to 11.29 W and the output power at 671 nm was increased from 0.141 W to 0.3 W simultaneously, as shown in Fig. 3. When the temperature of LBO was controlled at 29.04 °C, the best conversion efficiency of ICSHG was achieved with nonlinear conversion coefficient of $6.7*10^{-12}$ m^2/W, as shown by the circle in Fig. 1. When the LBO temperature was further tuned from 29.04 °C to 26 °C, the critical value of K for the sufficient condition of SLM operation was reached again. In the temperature range between 29.04 °C and 26 °C, the laser was also in SLM operation. Once the LBO temperature was controlled below 26 °C, the laser was in MLM operation. Consequently, at the output transmission of 7%, the region of LBO temperature ensuring stable SLM operation was 26 °C ~32 °C. Furthermore, at the output transmissions of 4% and 10%, the regions of LBO temperature ensuring stable SLM operation were 25.25 °C ~33 °C and 26.5 °C ~31.25 °C, respectively.
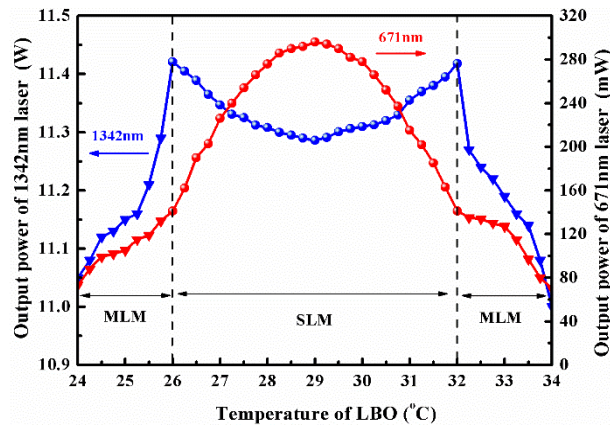

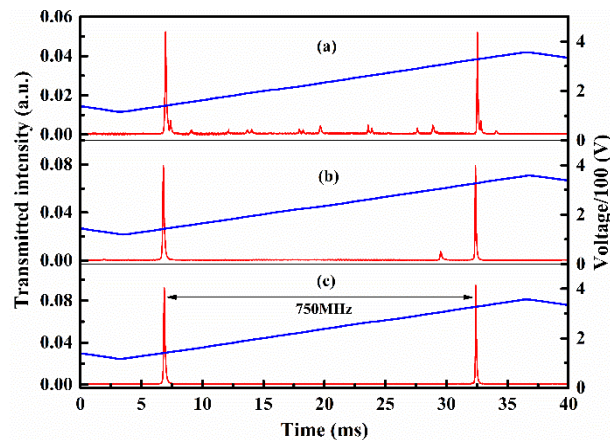Fig. 3. Output powers of 1342 nm and 671 nm laser versus the temperature of LBO.

Fig. 4. Transmitted intensity of the scanned F-P interferometer at an output transmission of 7% and different LBO temperatures (a) 39.5 °C, (b) 32.5 °C and (c) 29.04 °C.

When the LBO temperature was controlled at the optimum value of 29.04 °C and at an incident pump power of 50 W, the output powers of the stable cw SLM Nd:YVO$_4$ laser at 1342 nm and 671 nm versus the output transmissions are illustrated in Fig. 5. The triangles and diamonds are the experimental data. When the OC with transmission of 4% was used, the measured powers of 1342 nm and 671 nm lasers were 8.4 W and 0.39 W. When the OC with transmission of 10% was used, the measured powers of 1342 nm and 671 nm lasers were 11 W and 0.11 W. The solid curves in Fig. 5 are the theoretical predictions with ETU and ESA

taken into account, which show good agreement with the experiment data. As a comparison, the dashed curves in Fig. 5 are the theoretical predictions without ETU and ESA. It can be seen, the presence of ETU and ESA significantly reduces the powers of the laser, and makes the optimum output transmission moving towards lower value.
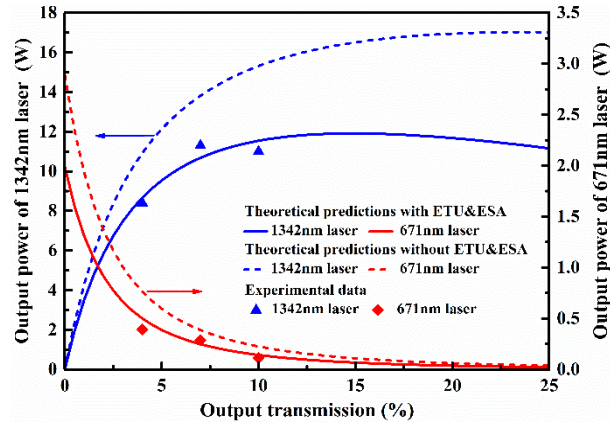

Fig. 5. Output powers of 1342 nm and 671 nm lasers versus transmission of output coupler.

When an OC with the optimum transmission of 7% was used, a dual-wavelength cw SLM laser exhibited 1342 nm laser power of 11.3 W, 671 nm laser power of 0.3 W, and excellent power and frequency stabilities was fabricated. Figure 6(a) and 6(b) show the measured fluctuations of the power and frequency of the 1342 nm laser operating at an average output power of 11.3 W, respectively. It can be seen, there is no mode hopping during a given three hours, the power stability is better than $\pm$ 0.5% and the frequency deviation is less than $\pm$ 88 MHz. Furthermore, the beam quality of the 1342 nm laser operating at an output power of 11.3 W was measured using a laser beam analyzer (Model: M2SETIR, Thorlabs), as shown in Fig. 7. The beam quality factors of the 1342 nm laser were $M_x^2 = 1.05$ and $M_y^2 = 1.07$.
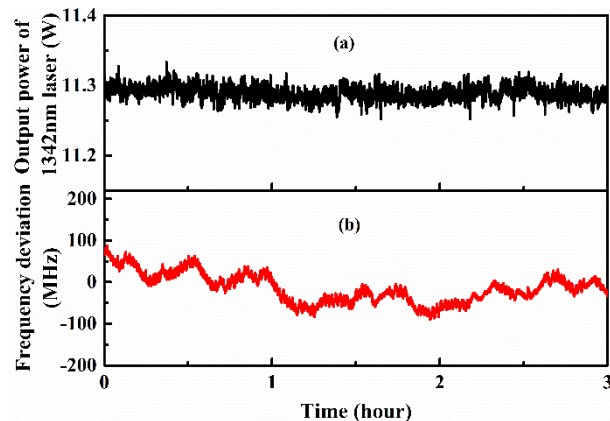

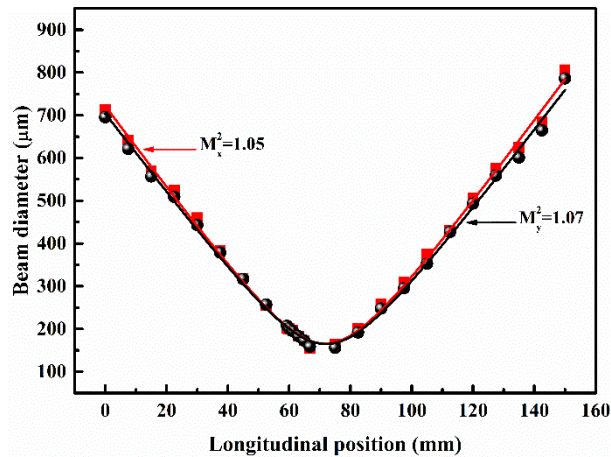Fig. 6. Measured fluctuations of the power and frequency of the 1342 nm laser.

Fig. 7. Measured beam quality of the 1342 nm laser.

5. Conclusions

We have presented a universal model about the sufficient condition of stable SLM operation for a high power unidirectional ring laser. Based on the model, the critical value of K as a function of T_{oc}, which denotes the sufficient condition for a high power cw Nd:YVO$_4$ laser operating at 1342 nm with ETU and ESA taken into account, is simulated. Using a unidirectional travelling-wave cavity configuration, a dual-wavelength Nd:YVO$_4$ laser at 1342 nm and 671 nm was fabricated. Then the influences of the LBO temperature and output transmission on the output characteristics and the SLM operation region of the laser were experimentally studied at a pump power of 50 W. When the OC with the optimum transmission of 7% was used, the region of LBO temperature ensuring stable SLM operation for the high power cw Nd:YVO$_4$ laser at 1342 nm was 26 °C ~32 °C. When the LBO temperature was controlled at 29.04 °C, perfect phase matching of SHG was achieved, and a stable SLM laser delivering 1342 nm output power of 11.3 W and 671 nm output power of 0.3 W was demonstrated with no mode hopping. The measured power stability and frequency fluctuation of the laser were better than ± 0.5% and less than ± 88 MHz during a given three hours, respectively. The beam quality factors of the 1342 nm laser operating at an output power of 11.3 W were $M_x^2 = 1.05$ and $M_y^2 = 1.07$. Note that good agreements are obtained between the experimental results and theoretical predictions of the dependence of laser powers on output transmission, as well as of longitudinal mode structure on LBO temperature, all of which give a direct validation of the universal model. Consequently, the theoretical model can be employed as a useful tool for the design of the high power SLM laser.

Funding